Static and Dynamic Characteristics in Levitating X-Y Transporter Using HTS Bulks

著者	津田　理
journal or publication title	IEEE Transactions on Applied Superconductivity
volume	12
number	1
page range	911-914
year	2002
URL	http://hdl.handle.net/10097/46517

doi: 10.1109/TASC.2002.1018548

Static and Dynamic Characteristics in Levitating X–Y Transporter Using HTS Bulks

Y. Teranishi, H. Ueda, M. Tsuda, and A. Ishiyama

***Abstract*—High T_c superconducting bulk has been used for magnetic levitation systems such as flywheel energy storage system, noncontact transport system and so on. We have been investigating electromagnetic behaviors of HTS bulk to realize a X–Y (two-dimensional) magnetic levitating transporter without any fixed guides. We have investigated qualitatively the characteristics of lift and restoring force of an YBCO bulk for various field-cooling conditions and permanent-magnet arrangements. In this paper, we evaluated the most suitable conditions of air gap in field-cooling process and permanent-magnet arrangement through lift and restoring force measurements and numerical analysis by the finite element method (FEM) based on the current vector potential method. The characteristics of oscillation in the vertical direction of levitating X–Y transporter were investigated by the measurements of free and forced vibrations. The theoretical characteristics of the free and forced vibrations were compared with the experiments.**

***Index Terms*—Dynamic characteristic, FEM, HTS bulk, levitating transporter, static characteristic.**

I. Introduction

One of the advantages of magnetic levitation using high-temperature superconducting (HTS) bulk is that stable levitation can be achieved without any control systems. In the levitation system using HTS bulk, the restoring force by pining effect works on the bulk against the displacement due to some disturbances. Therefore, the levitation system can achieve stable levitation without any complex control systems. Expanding the view of application of HTS bulk to amusement field, we have investigated and developed a two-dimensional magnetic levitating device, which can move stably and freely in any directions of a X–Y plane. In such the levitating device of "levitating X–Y transporter," it is necessary to comprehend the static and dynamic characteristics, such as lift, levitation height and stability. Therefore, we have measured lift and restoring force of a disk-shaped YBCO bulk, displaced by a distance in lateral direction, for various field-cooling conditions and permanent-magnet arrangements in the previous paper [1]. Both the lift and the restoring force are closely related to air gap between permanent magnets and permanent-magnet arrangement in field-cooling process. In this paper, the most suitable conditions of the air gap in field- cooling process and the permanent-magnet arrangement are estimated through the measurement and analysis of the lift and the restoring force. The characteristics of oscillation in the vertical and lateral directions are also very important factor as a dynamic stability. We investigate the diminishing process of the oscillation amplitude in free-vibration process and measured the amplitude of oscillation in the levitating part (permanent magnet).

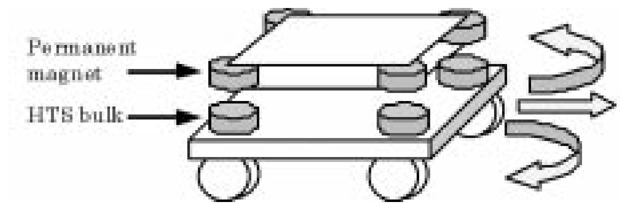

Fig. 1. Schematic drawing of "levitating X–Y transporter."

II. Concept of Levitating X–Y Transporter

Although HTS bulk has been applied to various types of magnetic levitation systems, most of them are used either in a static state or with one-dimensional movement. We have been developing a magnetic levitating device with two-dimensional movement, i.e., "levitating X–Y transporter." The concept of the levitating X–Y transporter is shown in Fig. 1. The transporter mainly composed of HTS bulks and permanent magnets (or HTS bulk magnets). The lower part and the upper part (levitating part) are connected magnetically; this means that the levitating part can move freely according to the lower part's movement without any contacts. The lower part is controlled by remote control system. Taking these advantages into account, we have been considering the application of the levitating X–Y transporter to not only industrial field but also entertainment or amusement field.

III. Static Characteristics: Lift and Restoring Force

Axial air gap between HTS bulk and permanent magnets is very important in magnetic levitating device and it depends on the weight of the levitating part and the magnitude of generated lift. We investigated the most suitable air gap in field-cooling condition using six types of permanent-magnet arrangements shown in Fig. 2. Influence of the arrangement on lift and lateral stability was also investigated experimentally. We measured restoring force in the lateral direction to evaluate the lateral stability.

Manuscript received September 25, 2001. This work was supported in part by Grant-in-Aid for basic research, Ministry of Education, Culture, Sports, Science and Technology, Japan.

Y. Teranishi, H. Ueda, and A. Ishiyama are with the Department of Electrical, Electronics and Computer Engineering, Waseda University, 3-4-1 Ohkubo, Shinjuku-ku, Tokyo 169-8555, Japan (e-mail: atsushi@mn.waseda.ac.jp).

M. Tsuda is with the Faculty of Engineering, Yamaguchi University, Tokiwadai, Ube, Yamaguchi 755-8611, Japan (e-mail: tsuda@po.cc.yamaguchi-u.ac.jp).

Publisher Item Identifier S 1051-8223(02)03852-6.

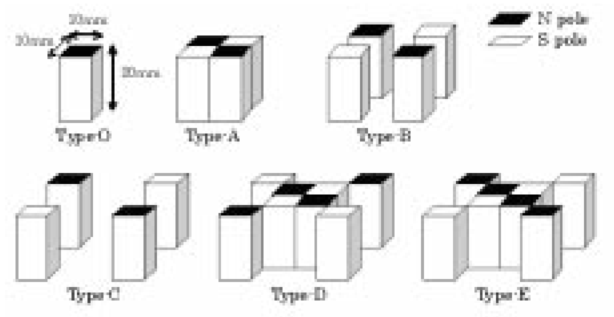

Fig. 2. Six types of permanent-magnet arrangements.

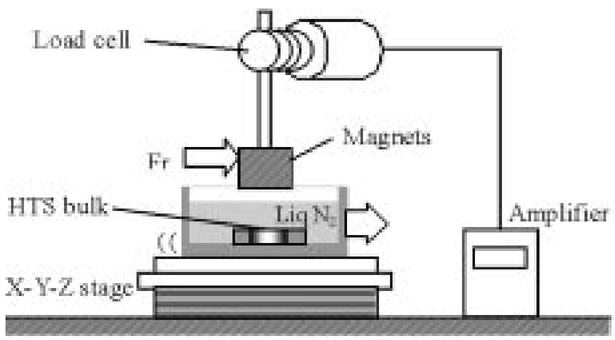

Fig. 3. Experimental setup for lift and restoring force measurements.

A. Experiments

1) Experimental Setup: A disk-shaped YBCO bulk with 46 mm in diameter and 15 mm in thickness was prepared for experiment. Rectangular-prism-shaped permanent magnets of Nd–Fe–B (10 mm $\times$ 10 mm $\times$ 20 mm) were adopted as the levitating part. The strength of magnetic flux density at the top surface of the permanent magnet is about 0.58 T. The distance between any two permanent magnets was set to be 10 mm in Type-B and 20 mm in Type-D, E and F. An experimental setup for lift and restoring force measurements is schematically drawn in Fig. 3. A load cell was used for the lift and restoring force measurements. The permanent magnets and the bulk were fixed to the load cell and the bottom of the vessel immersed in liquid nitrogen. The vessel can be moved smoothly in both axial and lateral directions.

2) Measurement: The most suitable air gap in field-cooling condition was evaluated using Type A and Type O. The air gap was changed in the range of 5 mm to 10 mm. The gap between the bulk and the permanent magnets was reduced at intervals of 1 mm until the minimum gap of 1 mm and then the gap was increased at the same intervals. Lift was measured at each gap in both increasing and decreasing processes. Restoring force was measured at intervals of 1 mm with maintaining the initial air gap between the bulk and the permanent magnets; the vessel with the bulk was moved in the lateral direction (x-direction).

B. Numerical Analysis

Supercurrent distribution within bulk is very important to evaluate electromagnetic behaviors of levitating X–Y transporter such as lift and restoring force. The critical state model and the finite element method (FEM) based on the current vector potential (T) method were adopted in this analysis. In order to avoid time-consuming in the calculation, we assumed that the bulk consists of several thin plates [2]. The governing equation using the scalar T for the thin plate approximation is written as follows:

$$\nabla \cdot \frac{1}{\sigma}\nabla T - \mu_0 \frac{\partial T}{\partial t} - \frac{\mu_0}{4\pi}\boldsymbol{n} \cdot \int_s \frac{\partial T}{\partial t}\nabla' \frac{1}{R}\, dS' = \frac{\partial B_0}{\partial t}, \quad (1)$$

where T is the current vector potential and the supercurrent density of J was obtained by:

$$J = \nabla \times T. \quad (2)$$

The critical current density, Jc, was assumed to be 5.0 $\times$ 10^7 A/m^2. The following techniques were used to determined supercurrent distribution according to the critical state model.

i) Initial conductivities in all elements are set in a sufficiently large value.
ii) J is obtained by solving equations (1) and (2).
iii) When the obtained current density is larger than the critical one, the equivalent conductivity is recalculated as follows:

$$\sigma_{new} = \sigma_{old} \frac{J_c}{|\boldsymbol{J}|}. \quad (3)$$

The above process is repeated until J does not exceed Jc in all elements.

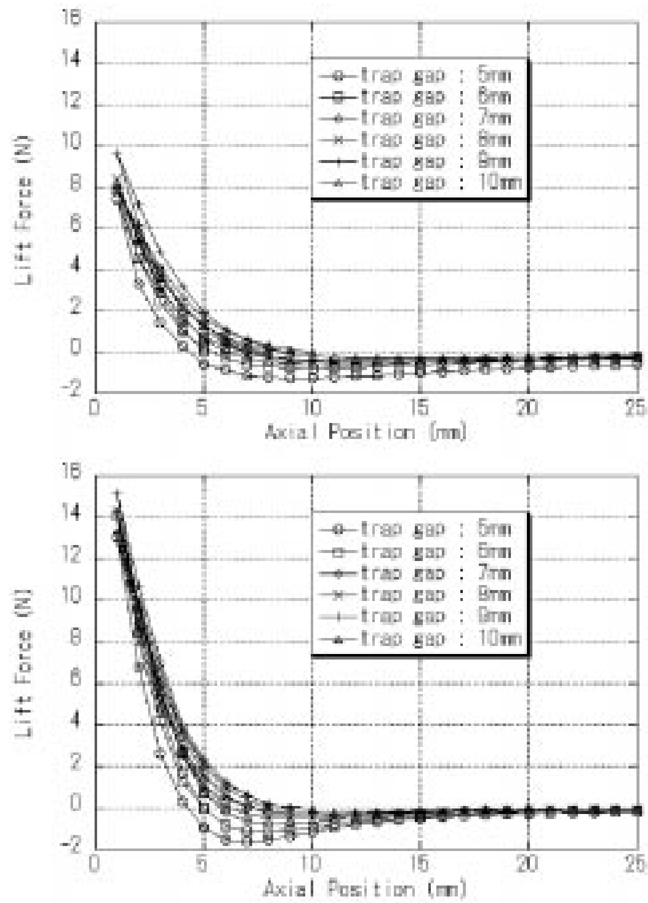

Fig. 4. Lift force in various air gap in field-cooling process. (Top) Type-O. (Bottom) Type-A.

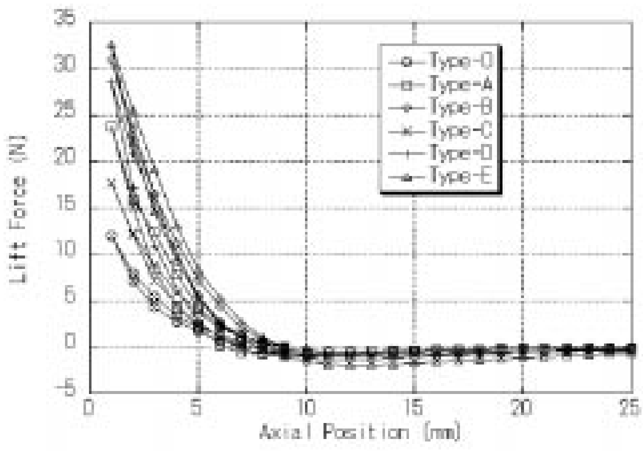

Fig. 5. Lift force in various permanent-magnet arrangements.

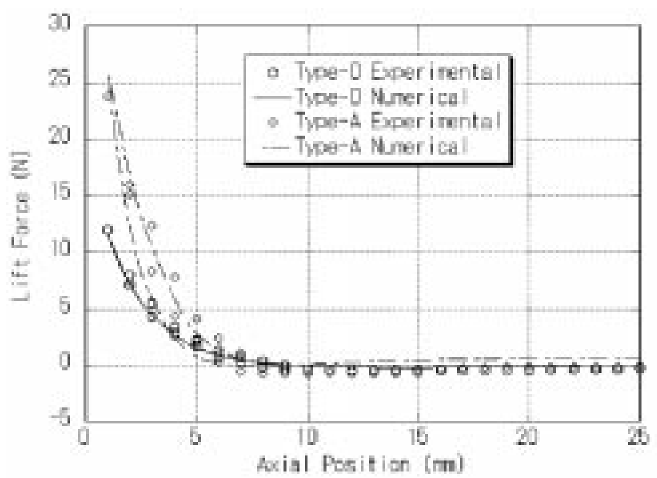

Fig. 6. Measured and computed lift force.

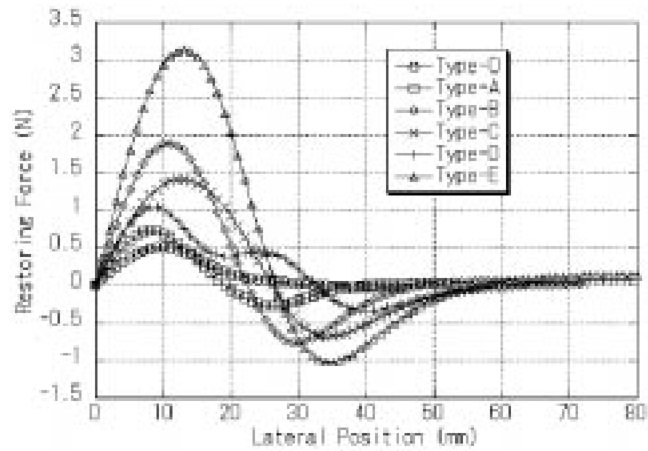

Fig. 7. Restoring force in various permanent-magnet arrangements.

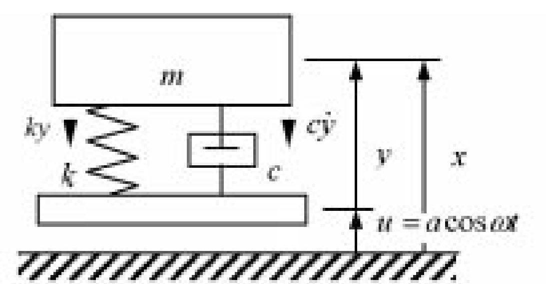

Fig. 8. Analytical model of forced vibration.

C. Results and Discussion

The experimental results of lift distribution of Type O and Type A as a function of air gap in field-cooling process are shown in Fig. 4. It may be considered that the most suitable air gap of this model was 9 mm due to generating the maximum lift at the air gap of 9 mm in both Type-O and Type-A. Using this air gap, we measured lift and restoring force of six types of permanent-magnet arrangements.

1) Lift: The measured lift distributions in the six types of permanent-magnet arrangements are shown in Fig. 5. Although lift has a tendency to increase with the number of permanent magnets, lift in Type B is larger than that in Type D; this means that not only the number of permanent magnets but also their locations are very important in their arrangements. It may be considered from the results of Type A, Type B and Type C that the most suitable distance between permanent magnets exists and depends on the size of the bulk. Type E generated the maximum lift in the six types of arrangements. The computed results of lift distribution in Type O and Type A are compared with experiments in Fig. 6. Agreements between the experiment and the analysis are good in both types.

2) Restoring Force: The experimental results of restoring force for various magnetic-pole arrangements are shown in Fig. 7. In comparison between Type B and Type C, the maximum restoring force in Type B was larger than that in Type C, while Type C is better than Type B in terms of the area in which restoring force works. The restoring force, as well as lift, in Type D was less than Type B. It can be considered as the reason that attractive and repulsive forces are mixed due to the complex permanent-magnet arrangement.

IV. DYNAMIC CHARACTERISTICS: OSCILLATION

In real operation of levitating X–Y transporter, the various kinds of forces may be applied to the levitating part and cause oscillation. Therefore, we investigated the characteristics of oscillation through the experiment and analysis of free and forced vibrations in the vertical direction of the levitating part. The diminishing process of the oscillation amplitude in free-vibration process was observed and the oscillation amplitude in the forced-vibration process was evaluated in experiment and analysis. Although it may be considered that levitating X–Y transporter has the nonlinear characteristics of oscillation due to HTS bulk, we assumed the experimental model as a simple linear system in the analysis. In the analytical model of vibration shown in Fig. 8, the amplitude of forced vibration, A, is obtained as follows:

$$A = \frac{\sqrt{1+\left(2\zeta\frac{\omega}{\omega_n}\right)^2}}{\sqrt{\left\{1-\left(\frac{\omega}{\omega_n}\right)^2\right\}^2+\left(2\zeta\frac{\omega}{\omega_n}\right)^2}}\,a \qquad (4)$$

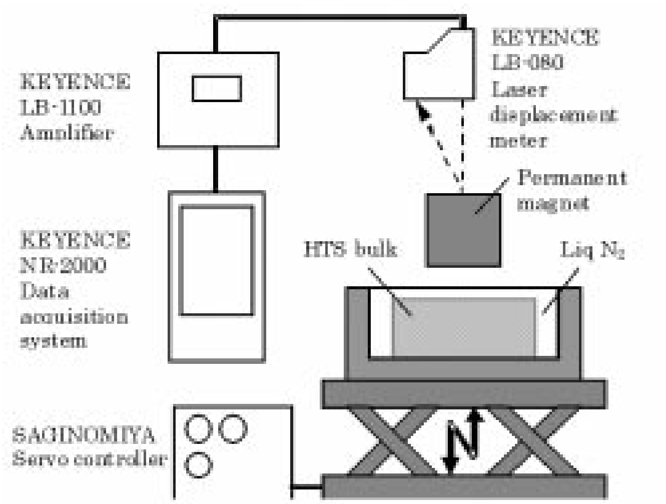

Fig. 9. Experimental setup for oscillation measurements.

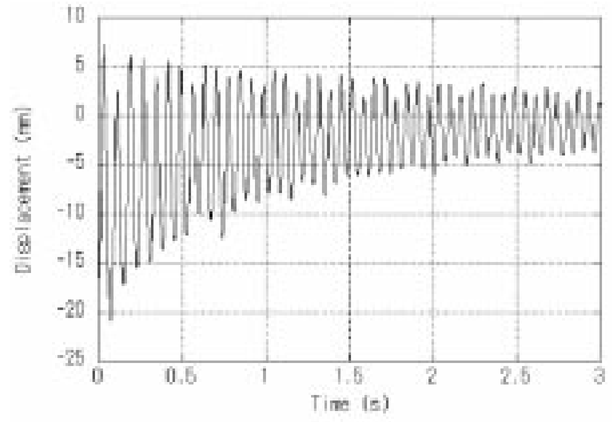

Fig. 10. Oscillation trace of levitating part in free vibration process.

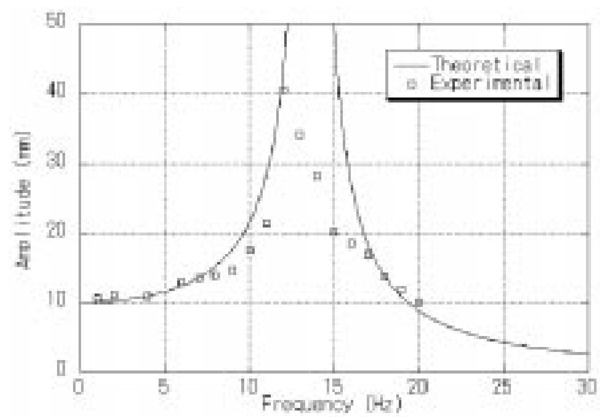

Fig. 11. Measured and calculated amplitude of oscillation.

where ω_n and ζ are the peculiar frequency and the attenuation ratio, respectively, m is the mass of levitating part, k and c are the spring and attenuation constants, respectively, and u is the displacement of vibrating source defined as $u = a\cos\omega t$.

A. Experimental Setup

The permanent-magnet arrangement of Type A was used in experiment and the bulk was field-cooled at the most suitable air gap of 9 mm. The displacement of levitating part was measured by a laser displacement meter. An experimental setup for forced-vibration measurement is shown in Fig. 9. The initial displacement from the equilibrium position was about 15 mm in the experiment of free vibration and the magnitude of vibrating source in forced vibration was 1 mm. The amplitude of the levitating part in forced vibration was measured at intervals of 1 Hz in the range of 1 Hz to 20 Hz.

B. Results and Discussion

The observed waveform of the free vibration is shown in Fig. 10. From the experimental result, ω_n and ζ of this system were estimated and the amplitude of forced vibration was calculated using (4). The measured and calculated results of the amplitude in forced vibration are shown in Fig. 11 as a solid line. Agreement between experiment and analysis is fair in the range of 10 Hz to 15 Hz. The error is caused by the assumption of linear-vibration model. The amplitude of oscillation jumped up between the frequency of 11 Hz and 12 Hz.

V. Conclusion

The static and dynamic characteristics of levitating X–Y transporter were investigated experimentally and analytically. In the static characteristics, the most suitable air gap in field-cooling process was evaluated by lift measurement and influence of permanent-magnet arrangements on lift and restoring force was investigated both experimentally and numerically. In the dynamic characteristics, free vibration in vertical direction was observed and the amplitude of forced vibration as a function of frequency was evaluated experimentally. Analytical approach using general linear-vibration model was also performed. It can be considered that the nonlinear characteristics of HTS bulk must be taken into account for the more rigorous investigation of the oscillation characteristics.

References

[1] Y. Sanagawa, *et al.*, "Characteristics of lift and restoring force in HTS bulk—Application to two-dimensional Maglev transporter," *IEEE Trans. Appl. Superconduct.*, vol. 11, no. 1, pp. 1797–1800, Mar. 2001.

[2] M. Uesaka, *et al.*, "Experimental and numerical analysis of three-dimensional high-Tc superconducting levitation system," *Int. J. Applied Electromagnetics in Material*, vol. 4, pp. 13–25, 1993.

[3] M. Tsuda, *et al.*, "'Electromaglev' ('active-maglev')-magnetic levitation of a superconducting disc with a DC field generated by electromagnets: Part 3. Theoretical results on levitation height and stability," *Cryogenics*, vol. 38, no. 7, p. 743, 1998.